



1 Have Aerosols Caused the Observed Atlantic
2 Multidecadal Variability?

3 Rong Zhang¹, Thomas L. Delworth¹, Rowan Sutton², Daniel L. R. Hodson²,
 Keith W. Dixon¹, Isaac M. Held¹, Yochanan Kushnir³, John Marshall⁴, Yi Ming¹,
 Rym Msadek¹, Jon Robson², Anthony J. Rosati¹, MingFang Ting³, Gabriel A. Vecchi¹

¹GFDL, NOAA, Princeton, NJ, USA

²NCAS-Climate, Dept. of Meteorology, University of Reading, Reading, UK

³Lamont-Doherty Earth Observatory, Columbia University, Palisades, NY, USA

⁴Dept. of Earth, Atmospheric and Planetary Sciences, MIT, Cambridge, MA, USA

Revised for Journal of Atmospheric Sciences

4 December 18, 2012

¹Corresponding author address: Rong Zhang, GFDL, NOAA, Princeton, NJ 08540. Email:

Rong.Zhang@noaa.gov

Abstract

5
6 Identifying the prime drivers of the twentieth-century multidecadal variability in the Atlantic
7 Ocean is crucial for predicting how the Atlantic will evolve in the coming decades and the re-
8 sulting broad impacts on weather and precipitation patterns around the globe. Recently Booth et
9 al (2012) showed that the HadGEM2-ES climate model closely reproduces the observed multi-
10 decadal variations of area-averaged North Atlantic sea surface temperature in the 20th century.
11 The multidecadal variations simulated in HadGEM2-ES are primarily driven by aerosol indirect
12 effects that modify net surface shortwave radiation. On the basis of these results, Booth et al
13 (2012) concluded that aerosols are a prime driver of twentieth-century North Atlantic climate
14 variability. However, here it is shown that there are major discrepancies between the HadGEM2-
15 ES simulations and observations in the North Atlantic upper ocean heat content, in the spatial
16 pattern of multidecadal SST changes within and outside the North Atlantic, and in the subpolar
17 North Atlantic sea surface salinity. These discrepancies may be strongly influenced by, and in-
18 deed in large part caused by, aerosol effects. It is also shown that the aerosol effects simulated in
19 HadGEM2-ES cannot account for the observed anti-correlation between detrended multidecadal
20 surface and subsurface temperature variations in the tropical North Atlantic. These discrepancies
21 cast considerable doubt on the claim that aerosol forcing drives the bulk of this multidecadal
22 variability.

1 Introduction

The observed 20th century multidecadal variations of area-averaged North Atlantic sea surface temperature (NASST) exhibit significant regional and hemispheric climate associations (Enfield et al. 2001; Sutton and Hodson, 2005; Knight et al. 2006; Zhang and Delworth, 2006; Zhang et al. 2007; Kushnir and Stein, 2010; Ting et al., 2011; Sutton and Dong, 2012). These variations are highly correlated with the multidecadal variations of the tropical North Atlantic SST and Atlantic hurricane activity (Goldenberg et al. 2001; Knight et al. 2006; Zhang and Delworth, 2006). In particular, tropical North Atlantic surface warming coincided with above-normal Atlantic hurricane activity during the 50-60's and the recent decade. These multidecadal NASST variations are often thought to be associated with Atlantic meridional overturning circulation (AMOC) variability (Delworth and Mann, 2000; Latif et al. 2004; Knight et al. 2005). On the other hand, some authors have suggested that they are at least in part driven by changes in the radiative forcing (Mann and Emanuel, 2006; Villarini and Vecchi, 2012). Various approaches have been proposed for quantitative attribution of NASST variations to a radiatively forced part and a part arising from AMOC variability (Kravtsov and Spannagle 2008; Ting et al. 2009; Zhang and Delworth 2009; Delsole et al. 2011; Wu et al. 2011; Terray 2012), and they show consistently that the role of internal variability cannot be ignored in multidecadal NASST variations.

Recently Booth et al 2012 (B12) showed that the HadGEM2-ES (Jones et al. 2011) climate model closely reproduces the amplitude and phase of the observed multidecadal variations of area-averaged NASST, especially over the 2nd half of the 20th century (Fig. 1). The multidecadal variations simulated in HadGEM2-ES are primarily driven by aerosol indirect effects that modify net surface shortwave radiation. On the basis of these results, B12 concluded that aerosols are a primary source of this multidecadal variability. However, B12 only compared the evolution of modeled and observed area-averaged NASST. In this study we show that there are major

47 discrepancies between the HadGEM2-ES simulations and many observed changes in the North
48 Atlantic. The discrepancies cast doubt upon the main conclusion of B12.

49 In section 2, the analysis methods and data used in this study are described. In sections
50 3-6 we compare the HADGEM2-ES simulations with observations over a range of variables.
51 The purpose of these comparisons is to assess more completely how well the HADGEM2-ES
52 simulations actually replicate the observed evolution of the North Atlantic over the 20th century.
53 In section 3 we examine North Atlantic upper ocean heat content. In section 4 we examine the
54 spatial patter of multidecadal SST changes. In section 5 we examine sea surface salinity (SSS)
55 in the North Atlantic. In section 6 we examine subsurface temperature anomalies in the Tropical
56 North Atlantic (TNA). Our conclusion is presented in section 7.

57 **2 Description of Method and Data**

58 In this study, the observed upper ocean heat content is derived from a yearly averaged dataset
59 of objectively analyzed ocean temperature anomalies since 1955 (Levitus et al. 2009). The ob-
60 served SSS data are from the pentadally averaged dataset of objectively analyzed ocean salinity
61 anomalies since 1957 (Boyer et al. 2005). The observed SST is based on the HADISST dataset
62 since 1871 (Rayner et al. 2003). The ensemble of four HadGEM2-ES historical simulations with
63 all external forcing (“All Forcings”) used in B12 are downloaded from the CMIP5 model output
64 archive at <http://cmip-gw.badc.rl.ac.uk>. The ensemble of three “Constant Aerosols” HadGEM2-
65 ES historical simulations (same as the first three members of the “All Forcings” except that an-
66 thropogenic aerosol emissions are fixed at 1860 levels) was provided to us by Ben Booth and Paul
67 Halloran from the Met Office Hadley Centre (MOHC). We assume linearity in the sense that the
68 ensemble mean difference (first three members) between “All Forcings” and “Constant Aerosols”
69 HadGEM2-ES historical simulations is assumed to represent the net response to anthropogenic

70 aerosols.

71 **3 North Atlantic Upper Ocean Heat Content**

72 Substantial warming trends in the upper ocean heat content have been observed in most ocean
73 basins since the middle of the 20th century (Domingues et al. 2008; Levitus et al. 2009). Gleck-
74 ler et al. (2012) using multiple observations (Domingues et al. 2008; Ishii and Kimoto 2009;
75 Levitus et al. 2009) and external forced and unforced simulations from phase 3 of the Coupled
76 Model Intercomparison Project (CMIP3), shows that the observed warming trend of upper ocean
77 heat content in the North Atlantic (and other basins) over the second half of the 20th century
78 is typically consistent with the response in these CMIP3 models to the sum of all external forc-
79 ing. The results suggest that changes in anthropogenic forcing (especially increasing greenhouse
80 gases) play an important role in the observed upper ocean warming trend.

81 In contrast to the observed heat content increase, the All Forcings HadGEM2-ES historical
82 simulations exhibit no trend in the area-averaged North Atlantic upper ocean heat content (0-
83 700m) between 1955 and 2004 (Fig. 2). The observed warming trend ($0.599 \times 10^{22} J/decade$)
84 for the period of 1955-2004 is clearly inconsistent with the modeled trend (Fig. 2). Over the
85 same period, the simulated trends for individual All Forcings ensemble members range from a
86 minimum of $-0.141 \times 10^{22} J/decade$ to a maximum of $0.118 \times 10^{22} J/decade$, all much smaller
87 than that observed. The HadGEM2-ES All Forcings simulations, which have strong aerosol
88 effects, suggest that there is no net radiatively forced warming in the North Atlantic upper ocean
89 over the 2nd half of the 20th century.

90 Using a different model (GFDL CM2.1), Delworth et al. (2005) shows that the surface waters
91 cooled by aerosol effects can penetrate into the subsurface ocean through subduction, and persist
92 in the subsurface for decades, thereby offsetting subsequent greenhouse gas induced subsurface

93 warming. The cooled surface waters can reduce vertical stratification in the ocean thus have
94 higher subduction rates (Marshall and Nurser, 1992). In HadGEM2-ES, over the 2nd half of
95 the 20th century, the simulated subsurface aerosol induced-cooling is evidently so strong that
96 it counteracted the subsurface greenhouse gas induced warming, resulting in a net subsurface
97 cooling in the North Atlantic. The subsurface cooling lags the surface response by decades
98 and even persists into the 1990's (not shown). On the contrary, in observations the subsurface
99 temperature is dominated by warm anomalies over this period (Domingues et al. 2008; Ishii and
100 Kimoto 2009; Levitus et al 2009).

101 In the ensemble-mean of the All Forcings HadGEM2-ES simulations, the simulated subsur-
102 face cooling trend offsets the surface warming trend, so there is almost no net heat content change
103 integrated over the North Atlantic upper ocean (0-700m) for the 2nd half of the 20th century. In
104 contrast, the ensemble of Constant Aerosols HadGEM2-ES historical simulations shows a clear
105 warming trend in the North Atlantic upper ocean heat content (Fig. 2). In B12, the Constant
106 Aerosols simulations are compared with All Forcings simulations to demonstrate the important
107 role of anthropogenic aerosols in NASST. Here the comparison between these two sets of simula-
108 tions also shows the important role of anthropogenic aerosols in causing the discrepancy between
109 simulated and observed trends in the North Atlantic upper ocean heat content. This discrepancy
110 with observations suggests that the aerosol effects are strongly overestimated over the North At-
111 lantic in HadGEM2-ES.

112 **4 Spatial Pattern of Multidecadal SST Changes**

113 The pattern of SST changes associated with the prominent cooling of NASST that occurred in the
114 late 1960s and 1970s is distinctly different in the HadGEM2-ES All Forcings simulations from
115 that seen in observations, both within and outside the North Atlantic (Fig. 3a,b). The observed

116 cooling is most pronounced in the subpolar and mid-latitude North Atlantic, while the model
117 shows a more extensive cooling in the tropical North Atlantic than seen in observations. The
118 observed abrupt cooling in the early 70's has the largest amplitude in the subpolar North Atlantic
119 (Thompson et al. 2010) and coincided with a rapid freshening of the subpolar North Atlantic
120 referred to as the "great salinity anomaly" (Dickson et al. 1988). This observed cooling in the
121 subpolar North Atlantic is largely underestimated in HadGEM2-ES All Forcings simulations.

122 Outside the North Atlantic, the HadGEM2-ES All Forcings simulations show excessive cool-
123 ing in the Barents Sea, North Pacific, tropical South Atlantic, Indian Ocean, and Southern Ocean
124 compared to that observed (Fig. 3a,b). The net response to anthropogenic aerosols (Fig. 3c,
125 difference between All Forcings and Constant Aerosols) is multidecadal cooling in most ocean
126 basins. In contrast, the observed multidecadal SST changes are characterized by a dipole pattern
127 in the Atlantic, suggestive of an important role for variations in the AMOC and related variations
128 in Atlantic heat transport (Zhang and Delworth, 2005; Ting et al. 2009; Robson et al. 2012).

129 This discrepancy is also reflected in the 10-year low-pass filtered time series of SST anomalies
130 averaged over the North Atlantic versus those averaged over the rest of the world ocean (Fig.
131 4). In observations, the low-pass filtered North Atlantic SST anomaly is characterized by a
132 pronounced multidecadal variability, whereas the low-pass filtered SST anomaly averaged over
133 the rest of the world ocean is dominated by an increasing trend with much weaker multidecadal
134 variability (Fig. 4a). In particular, for the period of 1961-1980, although the observed North
135 Atlantic SST was colder than the previous period of 1941-1960, the observed SST averaged over
136 the rest of the world ocean did not exhibit a cooling (Fig. 4a). However, in the HadGEM2-
137 ES All Forcings simulations, the low-pass filtered SST anomaly averaged over the rest of the
138 world ocean shows a strong multidecadal variability, and the abrupt post-1960 cooling simulated
139 in the North Atlantic SST is also present in the SST averaged over the rest of the world ocean
140 (Fig. 4b). Although the simulated low-pass filtered North Atlantic SST anomaly resembles

141 the observations (Fig. 4c), the simulated low-pass filtered SST anomaly averaged over the rest
142 of the world ocean is quite different from the observations (Fig. 4d). The observed low-pass
143 filtered SST anomaly averaged over the rest of the world ocean is outside the simulated ensemble
144 spread for most of the 20th century (Fig. 4d). The results consistently suggest that the time-
145 varying aerosols in HADGEM2-ES All Forcings simulations induce an unrealistic global scale
146 multidecadal variability.

147 **5 Subpolar North Atlantic Sea Surface Salinity anomalies**

148 The simulation of the subpolar North Atlantic sea surface salinity (SSS) in the HadGEM2-ES
149 All Forcings simulations also shows important differences to observations. In observations the
150 subpolar North Atlantic SSS anomalies exhibit multidecadal variations that are coherent and in
151 phase with variations in basin-mean and subpolar NASST (Fig. 5), with no long-term trend. In
152 contrast, the subpolar North Atlantic SSS simulated in HadGEM2-ES shows a salinification trend,
153 as well as variations that are largely out of phase with the observed subpolar NA SSS and also
154 out of phase with the simulated basin-mean NASST variations over the second half of the 20th
155 century (Fig. 5 and Fig. 4c). The simulated salinification trend in the subpolar North Atlantic is
156 consistent with the response to aerosol forcing as shown in a previous study using GFDL CM2.1
157 (Delworth and Dixon 2006). The Constant Aerosols ensemble shows no significant salinification
158 trend at the surface in the subpolar North Atlantic (Fig. 5), and the mean value of subpolar North
159 Atlantic SSS over the period 1871-2000 is 0.2 PSU lower in Constant Aerosols simulations than
160 that in All Forcings simulations, consistent with this interpretation.

161 The subpolar SSS changes are directly linked to changes in deep water formation and large-
162 scale ocean circulation (Curry et al. 1998). The discrepancies in subpolar North Atlantic SSS
163 again suggest the aerosol effects are strongly overestimated in HadGEM2-ES. In contrast, the ob-

164 served coherent relationships between subpolar North Atlantic SSS/SST and basin-mean NASST
165 variations are consistent with the notion that the AMOC plays an important role in the Atlantic
166 multidecadal variability, as suggested by a number of climate model based studies (Delworth, et
167 al. 1997; Robson et al. 2012).

168 **6 Detrended Tropical North Atlantic Subsurface Tempera-** 169 **ture Anomalies**

170 Zhang (2007b) showed that the observed multidecadal variations of Tropical North Atlantic
171 (TNA) SST are strongly anticorrelated with those of TNA subsurface ocean temperature, with
172 long-term trends removed. Therefore, mechanisms that are proposed to explain the observed
173 multidecadal TNA SST variations should also be consistent with the observed anticorrelations
174 between TNA surface and subsurface temperature variations. Further, we note that model re-
175 sults in Zhang (2007b) suggest that this out of phase relationship between surface and subsurface
176 ocean temperature in the Tropical North Atlantic is a distinctive feature of AMOC variations.

177 Here we apply the same analyses as in Zhang (2007b) to the linear detrended TNA SST
178 anomalies and subsurface temperature anomalies from the HadGEM2-ES All Forcings ensemble.
179 The analyses here are not aimed to the question whether aerosol effects have been overestimated
180 in the HadGEM2-ES, thus are different from the other discrepancies discussed in Section 3-5.
181 The analyses in this Section are to test the hypothesis that the aerosol mechanism can account
182 for the observed anticorrelation between the detrended TNA surface and subsurface temperature
183 variations. The analyses are compared with the detrended observations and the ensemble of water
184 hosing experiments using a CMIP3 coupled climate model (GFDL CM2.1, Delworth et al. 2006).
185 In the ensemble of water hosing experiments, a strong freshwater flux anomaly is uniformly
186 distributed over the subpolar North Atlantic for 60 years, and the AMOC weakens gradually in

187 response. The changes in TNA temperature (surface and subsurface) in response to the freshwater
188 forcing are indicative of the AMOC effects in the TNA. There is no need for detrending for the
189 ensemble of water hosing experiments, as all radiative forcings are held constant in this ensemble.

190 As shown in Zhang (2007b), in the water hosing experiments the AMOC-induced anticorre-
191 lated changes between the TNA surface and subsurface temperature are clearly apparent in the
192 spatial regression pattern of surface and subsurface temperature anomalies onto the TNA SST
193 anomaly (Fig. 6a,d). The detrended observations also show anticorrelated changes, i.e. positive
194 regression coefficients over most of the TNA surface and negative regression coefficients over
195 most of the TNA subsurface (Fig. 6b,e). In contrast, the ensemble mean detrended results from
196 the HadGEM2-ES All Forcings simulations show positive regression coefficients over the surface
197 TNA, but almost no signals over most of the subsurface TNA (Fig. 6c,f). The vertical structure of
198 the regression of the TNA ocean temperature anomalies onto the TNA SST anomaly (Fig. 6g,h,i)
199 shows similar results. The TNA SST anomalies induced by aerosol forcing could slowly diffuse
200 or subduct into the subsurface, but there is no obvious mechanism by which the time-varying
201 aerosol forcing could give rise to subsurface temperature changes of opposite polarity to the SST
202 anomalies on these time scales. Hence aerosol effects simulated in this All Forcings ensemble
203 cannot account for the anticorrelated multidecadal SST and subsurface temperature variations in
204 the detrended observations for the TNA.

205 In water hosing experiments, two dominant processes are excited rapidly by the AMOC
206 weakening - surface southward displacements of the Atlantic ITCZ and subsurface thermocline
207 deepening through the propagation of oceanic waves. These processes act together to produce
208 opposite changes between the TNA surface and subsurface temperature (Zhang, 2007b). Simi-
209 lar AMOC-induced anticorrelated surface and subsurface TNA variations have also been found
210 in NCAR CCSM3 coupled model simulations (Chiang et al. 2008). A recent study using high-
211 resolution temperature records of the last deglacial transition from a southern Caribbean sediment

212 core also shows that warmer subsurface temperatures correspond to colder surface temperatures
213 and a weaker AMOC during the Younger Dryas (Schmidt et al. 2012). The analyses here suggest
214 that the observed anticorrelated multidecadal TNA SST and subsurface temperature variations
215 are consistent with the mechanism of AMOC variations, and inconsistent with the dominance
216 of changes in aerosols. For example, during the 70-80's, the observed detrended TNA surface
217 cooling and subsurface warming is consistent with a weaker strength of the AMOC when the
218 Labrador Sea deep water formation was substantially reduced due to the “great salinity anomaly”
219 events (Curry et al. 1998).

220 We have shown here that out of phase temperature variations are seen between the surface
221 and subsurface in the TNA for both observations and in model simulations of AMOC changes.
222 In contrast, this out of phase behavior is not seen in the HADGEM2-ES simulations. This sug-
223 gests that the aerosol mechanism cannot account for the observed anticorrelated multidecadal
224 TNA SST and subsurface temperature variations, regardless of whether the aerosol effects are
225 overestimated. This discrepancy is inconsistent with the interpretation that aerosol forcing drives
226 the bulk of the observed Atlantic multi-decadal variability.

227 **7 Conclusions**

228 In this paper we have tried to present a broad, multivariate comparison between the observed
229 changes and those simulated in the HADGEM2-ES model. In this comparison, we have included
230 not only SST in the North Atlantic, but also sea surface salinity and subsurface ocean temperature,
231 as well as the vertical structure of temperature variations.

232 In summary, key aspects of the HadGEM2-ES simulation exhibit substantial discrepancies
233 with observations. Discrepancies are seen in the North Atlantic upper ocean heat content, in the
234 spatial pattern of multidecadal SST changes within and outside the North Atlantic, and in the

235 subpolar North Atlantic sea surface salinity. These discrepancies are largely attributable to what
236 appears to be excessively strong aerosol effects. It is also shown that the aerosol effects simulated
237 in the HadGEM2-ES All Forcings ensemble cannot account for the anticorrelated multidecadal
238 SST and subsurface temperature variations of the detrended observations for the tropical North
239 Atlantic.

240 Anthropogenic and natural aerosols have likely played some role in forcing the observed At-
241 lantic multidecadal variability (Evan et al. 2009; Chang et al. 2011; Villarini and Vecchi, 2012),
242 and understanding the magnitude of their influence on the North Atlantic SSTs remains a key
243 challenge. Aerosol indirect effects remain poorly understood owing to difficulties in representing
244 sub-grid cloud processes in global climate models (Lohmann et al. 2010). The discrepancies
245 pointed out in this paper call into question the claim of B12 that aerosols have been a domi-
246 nant forcing of observed Atlantic multidecadal variability and the realism of the HadGEM2-ES
247 simulations of the aerosol influence on North Atlantic SST.

248 We single out the HadGEM2-ES model for this critique to counterbalance the claims in Booth
249 et al (2012) for the dominance of aerosol forcing for multi-decadal Atlantic variability. Whether
250 it is possible for a model to exhibit comparably large indirect aerosol effects without the incon-
251 sistencies with observations outlined here remains to be seen.

252 **Acknowledgments.** We acknowledge the World Climate Research Programme’s Working Group
253 on Coupled Modelling, which is responsible for CMIP, and we thank the Met Office Hadley Cen-
254 tre (MOHC) for producing and making available the HadGEM2-ES All Forcings historical sim-
255 ulations. For CMIP the U.S. Department of Energy’s Program for Climate Model Diagnosis and
256 Intercomparison provides coordinating support and led development of software infrastructure in
257 partnership with the Global Organization for Earth System Science Portals. We thank Ben Booth
258 and Paul Halloran from the Met Office Hadley Centre (MOHC) for proving us the ensemble of
259 Constant Aerosols HadGEM2-ES historical simulations.

References

- Booth, B. B. B., Dunstone, N. J., Halloran, P. R., Andrews, T. and Bellouin, N. Aerosols implicated as a prime driver of twentieth-century North Atlantic climate variability. *Nature*, 484, 228-232 (2012).
- Boyer, T. P., Levitus, S., Antonov, J. I., Locarnini, R. A., and Garcia, H. E. Linear trends in salinity for the World Ocean, 1955-1998, *Geophysical Research Letters*, 32, L01604, doi:10.1029/2004GL021791 (2005).
- Chang, C. Y., Chiang, J. C. H. Wehner, M. F. Friedman, A. Ruedy, and R. Sulfate aerosol control of tropical Atlantic climate over the 20th century. *J. Climate*, 24, 25402555 (2011).
- Chiang, J. C. H., W. Cheng, and C. M. Bitz: Fast teleconnections to the tropical Atlantic sector from Atlantic thermohaline adjustment. *Geophysical Research Letters*, 35, L07704, doi:10.1029/2008GL033292 (2008)
- Curry, R. G., M. S. McCartney, and T. M. Joyce, Oceanic transport of subpolar climate signals to mid-depth subtropical waters. *Nature*, 391, 575-577 (1998).
- DelSole, Timothy, Michael K. Tippett, Jagadish Shukla, A Significant Component of Unforced Multidecadal Variability in the Recent Acceleration of Global Warming. *J. Climate*, 24, 909-926 (2011).
- Delworth, T. L., and M. E. Mann, Observed and simulated multidecadal variability in the Northern Hemisphere, *Clim. Dyn.*, 16, 661-676 (2000).
- Delworth, T. L., Ramaswamy, V. and Stenchikov, G. The impact of aerosols on simulated ocean temperature and heat content in the 20th century. *Geophysical Research Letters*, 32, L24709, DOI:10.1029/2005GL024457 (2005).

282 Delworth, T. L. and Dixon K. W. Have anthropogenic aerosols delayed a greenhouse gas-
283 induced weakening of the North Atlantic thermohaline circulation? *Geophysical Research*
284 *Letters*, 33, L02606, DOI:10.1029/2005GL024980 (2006).

285 Delworth et al. GFDL's CM2 global coupled climate models. part I: Formulation and simulation
286 characteristics, *J. Clim.*, 19, 643-674 (2006)

287 Domingues, C. et al. (2008) Improved estimates of upper-ocean warming and multi-decadal
288 sea-level rise. *Nature*, 453, 1091-1094.

289 Dickson, R. R., Meincke, J., Malmber, S. A. and Lee, A. J. The "great salinity anomaly" in the
290 northern North Atlantic 1968-1982. *Prog. Oceanogr.* 20, 103151 (1988).

291 Evan, A. T., Vimont, D. J., Heidinger, A. K., Kossin, J. P. and Bennartz, R. The role of aerosols
292 in the evolution of tropical North Atlantic Ocean temperature anomalies. *Science*, 324,
293 778-781 (2009).

294 Enfield, D. B., A. M. Mestas-Nuñez, and P. J. Trimble, The Atlantic Multidecadal Oscillation
295 and its relation to rainfall and river flows in the continental U.S., *Geophys. Res. Lett.*, 28,
296 2077-2080 (2001).

297 Gleckler, B. D. Santer, C. M. Domingues, D. W. Pierce, T. P. Barnett, J. A. Church, K. E. Tay-
298 lor, K. M. AchutaRao, T. P. Boyer, M. Ishii, P. M. Caldwell (2012). Human-induced global
299 ocean warming on multidecadal timescales. *Nature Climate Change*, DOI: 10.1038/ncli-
300 mate1553

301 Goldenberg, S. B., C. W. Landsea, A. M. Mestas-Nuñez, and W. M. Gray (2001), The recent
302 increase in Atlantic hurricane activity: Causes and implications, *Science*, 293, 474-479.

303 Kravtsov, S., and C. Spannagle, Multi-decadal climate variability in observed and modeled
304 surface temperatures, *J. Clim.*, 21, 1104-1121 (2008).

305 Ishii, M. and Kimoto, M. (2009), Reevaluation of historical ocean heat content variations with
306 time-varying XBT and MBT depth bias corrections. *J. Oceanogr.* 65, 287-299.

307 Jones C. D. et al. The HadGEM2-ES implementation of CMIP5 centennial simulations. *Geosci.*
308 *Model Dev.*, 4, 543-570 (2011).

309 Knight, J. R., R. J. Allan, C. K. Folland, M. Vellinga, and M. E. Mann, A signature of persis-
310 tent natural thermohaline circulation cycles in observed climate, *Geophys. Res. Lett.*, 32,
311 L20708, doi:10.1029/2005GL024233 (2005).

312 Knight, J. R., C. K. Folland, and A. A. Scaife, Climate impacts of the Atlantic Multidecadal
313 Oscillation, *Geophys. Res. Lett.*, 33, L17706, doi:10.1029/2006GL026242 (2006).

314 Kushnir, K. and M. Stein, North Atlantic influence on 19th-20th century rainfall in the Dead
315 Sea watershed, teleconnections with the Sahel, and implication for Holocene climate fluc-
316 tuations. *Quaternary Science Reviews*, 29: doi:10.1016/j.quascirev.2010.09.004 (2010).

317 Latif et al. Reconstructing, Monitoring, and Predicting Multidecadal-Scale Changes in the
318 North Atlantic Thermohaline Circulation with Sea Surface Temperature. *J. Climate*, 17,
319 1605-1614 (2004).

320 Levitus S. et al. Global ocean heat content 1955-2008 in light of recently revealed instrumen-
321 tation problems. *Geophysical Research Letters*, 36, L07608, doi:10.1029/2008GL037155
322 (2009).

323 Lohmann, U. et al. Total aerosol effect: radiative forcing or radiative flux perturbation? *Atmos.*
324 *Chem. Phys.*, 10, 3235-3246, doi:10.5194/acp-10-3235-2010 (2010).

325 Mann, M. E., and K. A. Emanuel, Atlantic hurricane trends linked to climate change, *Eos Trans.*
326 *AGU*, 87, 233 (2006).

327 Marshall, J. C. and Nurser, A. J. G. Fluid Dynamics of Oceanic Thermocline Ventilation, *J.*
328 *Phys. Oceanogr.*, 22, 583-595, 1992.

329 Rayner, N. A. et al. A. Global analyses of sea surface temperature, sea ice, and night marine air
330 temperature since the late nineteenth century. *Journal of Geophysical Research*, 108, 4407
331 10.1029/2002JD002670 (2003).

332 Robson, J., Sutton, R., Lohmann, K., Smith, D. and Palmer, M. Causes of the Rapid Warming
333 of the North Atlantic ocean in the mid 1990s. *J. Climate*. doi:10.1175/JCLI-D-11-00443.1,
334 In Press (2012).

335 Schmidt, M.W., Chang, P., Hertzberg, J.E., Them, T.R., Ji, L., and Otto-Bliesner, B.L. Impact
336 of Abrupt Deglacial Climate Change on Tropical Atlantic subsurface temperatures. *Pro-*
337 *ceedings of the National Academy of Sciences*, In Press, doi:10.1073/pnas.1207806109
338 (2012).

339 Sutton, R. T., and D. L. R. Hodson, Atlantic Ocean forcing of North American and European
340 summer climate, *Science*, 309, 115-118 (2005).

341 Sutton, R. T., and B. Dong, Atlantic Ocean influence on a shift in European climate in the 1990s,
342 *Nature Geoscience*, 5, 788-792 (2012).

343 Terray, L., Evidence for multiple drivers of North Atlantic multi-decadal climate variability.
344 *Geophys. Res. Lett.*, 39, L19712 (2012).

345 Ting, M.; Kushnir, Y.; Seager, R.; Li, C., Forced and Internal 20th Century SST Trends in the
346 North Atlantic, *Journal of Climate*, 22, 10.1175/2008JCLI2561.1 (2009).

347 Ting, M., Y. Kushnir, R. Seager and L. Cuihua, Robust features of Atlantic multi-
348 decadal variability and its climate impacts. *Geo. Res. Letters*, 38(L17705):
349 doi:10.1029/2011GL048712(2011).

350 Thompson, D.W. J., Wallace, J. M., Kennedy, J. J. and Jones, P. D. An abrupt drop in Northern
351 Hemisphere sea surface temperature around 1970. *Nature*, 467, 444-447 (2010).

352 Villarini, G. and G. A. Vecchi, Projected Increases in North Atlantic Tropical Cyclone Intensity
353 from CMIP5 Models. *J. Climate*, In Press, 2012.

354 Wu Z., N. E. Huang, J. M. Wallace, B. Smoliak, X. Chen, On the time-varying trend in global-
355 mean surface temperature. *Clim. Dyn.* 37, 759-773, DOI: 10.1007/s00382-011-1128-8
356 (2011).

357 Zhang, R. and Delworth, T. L. Simulated tropical response to a substantial weakening of the
358 Atlantic thermohaline circulation. *J. Climate*, 18, DOI:10.1175/JCLI3460.1 (2005).

359 Zhang, R., and T. L. Delworth, Impact of Atlantic multidecadal oscillations on India/Sahel rain-
360 fall and Atlantic hurricanes, *Geophys. Res. Lett.*, 33, L17712, doi:10.1029/2006GL026267
361 (2006).

362 Zhang, R., T. L. Delworth, and I. M. Held, Can the Atlantic Ocean drive the observed multi-
363 decadal variability in Northern Hemisphere mean temperature?, *Geophys. Res. Lett.*, 34,
364 L02709, doi:10.1029/2006GL028683 (2007a).

365 Zhang, R., Anticorrelated multidecadal variations between surface and subsurface tropical
366 North Atlantic. *Geophysical Research Letters*, 34, L12713, doi:10.1029/2007GL030225
367 (2007b).

368 Zhang, R., and T. L. Delworth (2009), A new method for attributing climate variations over the
369 Atlantic Hurricane Basin's main development region, *Geophys. Res. Lett.*, 36, L06701,
370 doi:10.1029/2009GL037260.

Figure Captions

1. Area-averaged North Atlantic SST (NASST) Anomaly (75-7.5°W, 0-60°N), adapted from Fig. 1b in Booth et al. (2012). Red Line: ensemble mean of HadGEM2-ES historical simulations with all external forcing (“All Forcings”). Black Line: Observations (HadISST). Orange shading: 1 std of ensemble spread of HadGEM2-ES All Forcings. All anomalies are relative to 1871-2000 mean.
2. North Atlantic upper ocean heat content anomaly. Red line: area-averaged North Atlantic upper ocean heat content anomaly (0-700m, 75-7.5°W, 0-60°N) from ensemble mean of HadGEM2-ES All Forcings simulations. Yellow shading: 1 std of ensemble spread of All Forcings. Green Line: ensemble mean from Constant Aerosols historical simulations. Black Line: observations. All anomalies are relative to 1955-2004 mean. The dash lines are linear trends for the respective variables. The 1955-2004 trend is $0.599 \times 10^{22} J/decade$ for observations and $0.003 \times 10^{22} J/decade$ for HadGEM2-ES All Forcings ensemble mean.
3. SST differences between the North Atlantic cold period (1961-1980) and the North Atlantic warm period (1941-1960). (a) Observations (b) HadGEM2-ES All Forcings ensemble mean (c) Ensemble mean difference between HadGEM2-ES All Forcings and Constant Aerosols.
4. Comparison of 10-Year low-pass filtered NASST anomaly (blue) with 10-Year low-pass filtered SST anomaly averaged for the Rest of the World Ocean (red). (a) Observations (HadISST) (b) ensemble mean of HadGEM2-ES All Forcings. Green shading: 1 std of ensemble spread for low-pass filtered NASST anomaly; yellow shading: 1 std of ensemble spread for low-pass filtered SST anomaly averaged for the Rest of the World Ocean. (c) low-pass filtered NASST anomaly from HadGEM2-ES All Forcings (blue) and observations (blue dash line) (d) low-pass filtered SST anomaly averaged for the Rest of the World

395 Ocean from HadGEM2-ES All Forcings (red) and observations (red dash line). The color
396 shadings in (c,d) are the same as in (b).

397 5. Subpolar North Atlantic SSS anomaly (60°W - 0°E , 50 - 65°N). Red Line: subpolar North
398 Atlantic SSS anomaly from ensemble mean of HadGEM2-ES All Forcings simulations;
399 Blue Line: subpolar North Atlantic SSS anomaly from ensemble mean of HadGEM2-ES
400 Constant Aerosols simulation. Black Line: observed subpolar North Atlantic SSS anomaly
401 (pentadally averaged), relative to 1957-2000 mean. Yellow Line: observed subpolar North
402 Atlantic SST anomaly, relative to 1871-2000 mean. Green Line: observed North Atlantic
403 basin-averaged NASST anomaly, relative to 1871-2000 mean. Thin red line: marking the
404 0.2PSU difference in the climatological mean subpolar North Atlantic SSS over the entire
405 period 1871-2000 between HadGEM2-ES All Forcings and Constant Aerosols.

406 6. Regression coefficients of SST anomaly (a,b,c), subsurface ocean temperature anomaly
407 ($z=400$) (d,e,f), and averaged Tropical North Atlantic (TNA) ocean temperature anomaly
408 at different depths (g,h,i) onto the time series of the TNA SST anomaly, corresponding to
409 1 standard deviation of the TNA SST anomaly. (a, d, g) ensemble mean from water hosing
410 experiments using GFDL CM2.1, year 1-60. (b, e, h) Using 10-year low-pass filtered
411 observed data (OBS, 1955-2000) (c, f, i) Using 10-year low-pass filtered modeled ensemble
412 mean from HadGEM2-ES All Forcings simulations, 1955-2000. The long-term trends have
413 been removed for OBS and HadGEM2-ES. The brown box shows the TNA domain (0 -
414 14°N and 70°W - 0°E) that is used for area average. (g,h,i) are normalized by the maximum
415 absolute value of each regression respectively, and the green shading covers depths that
416 are not statistically significant at the 90% level of non-zero correlation using the 2-tailed
417 Student's t -test.

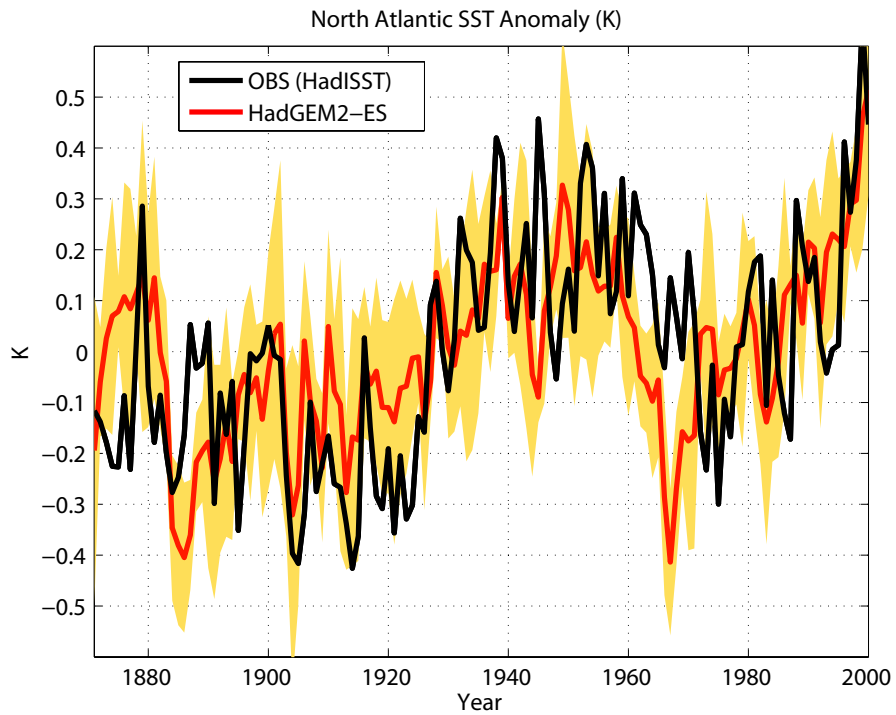


Figure 1: Area-averaged North Atlantic SST (NASST) Anomaly ($75\text{-}7.5^{\circ}\text{W}$, $0\text{-}60^{\circ}\text{N}$), adapted from Fig. 1b in Booth et al. (2012). Red Line: ensemble mean of HadGEM2-ES historical simulations with all external forcing (“All Forcings”). Black Line: Observations (HadISST). Orange shading: 1 std of ensemble spread of HadGEM2-ES All Forcings. All anomalies are relative to 1871-2000 mean.

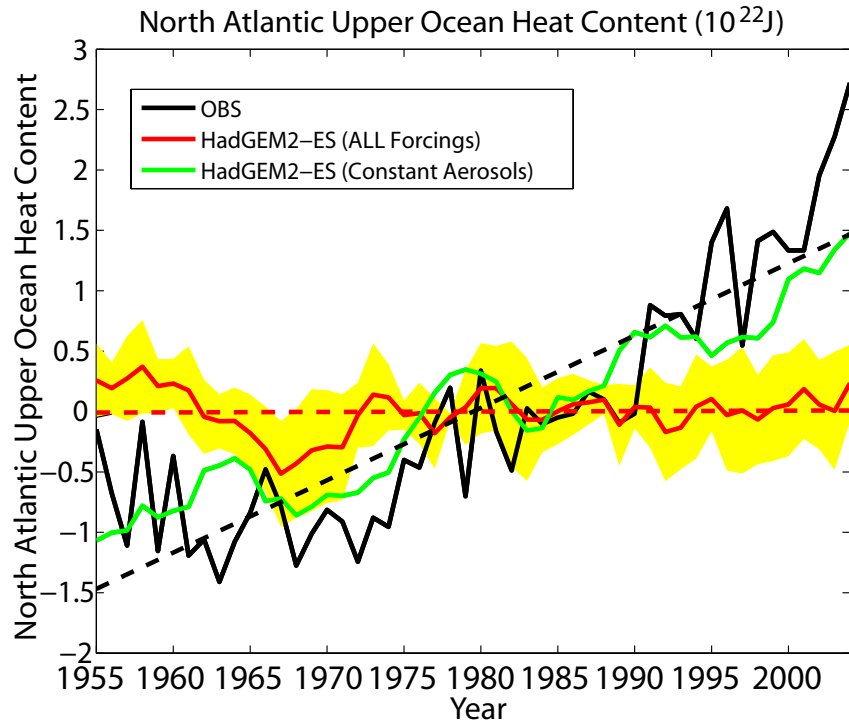


Figure 2: North Atlantic upper ocean heat content anomaly. Red line: area-averaged North Atlantic upper ocean heat content anomaly (0-700m, 75-7.5°W, 0-60°N) from ensemble mean of HadGEM2-ES All Forcings simulations. Yellow shading: 1 std of ensemble spread of All Forcings. Green Line: ensemble mean from Constant Aerosols historical simulations. Black Line: observations. All anomalies are relative to 1955-2004 mean. The dash lines are linear trends for the respective variables. The 1955-2004 trend is $0.599 \times 10^{22}J/decade$ for observations and $0.003 \times 10^{22}J/decade$ for HadGEM2-ES All Forcings ensemble mean.

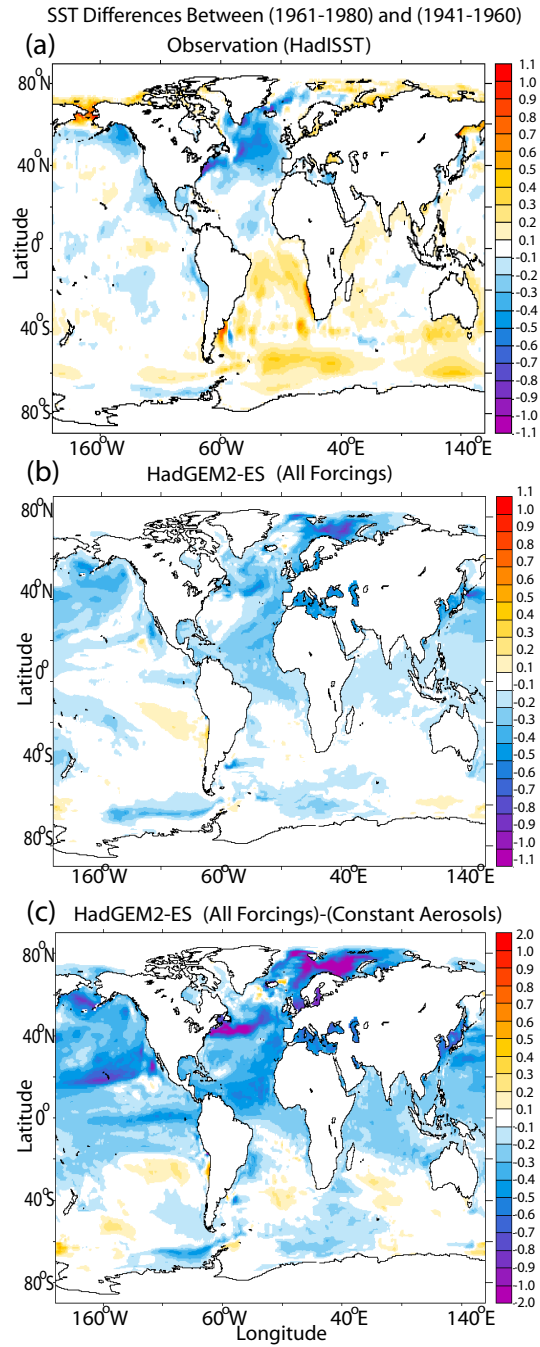


Figure 3: SST differences between the North Atlantic cold period (1961-1980) and the North Atlantic warm period (1941-1960). (a) Observations (b) HadGEM2-ES All Forcings ensemble mean (c) Ensemble mean difference between HadGEM2-ES All Forcings and Constant Aerosols.

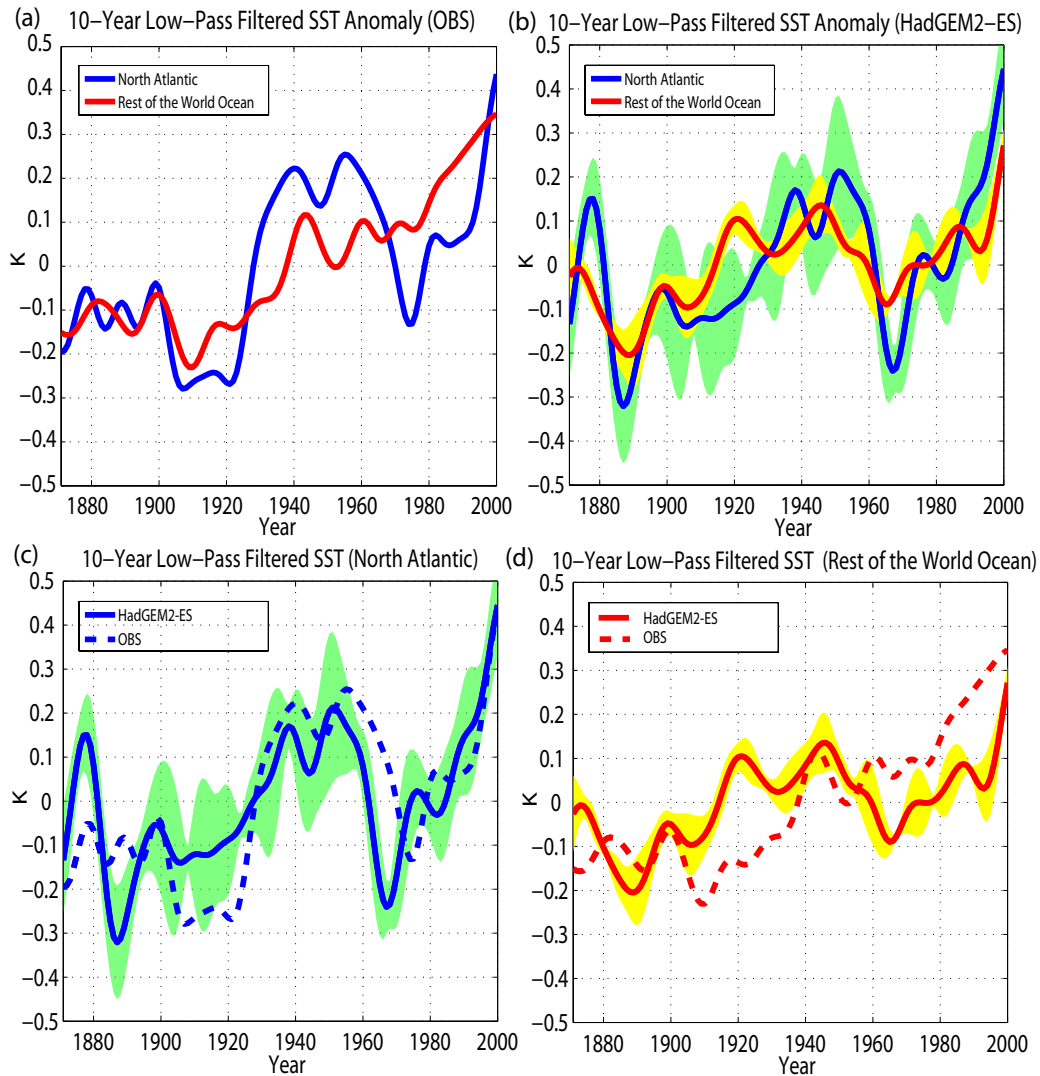


Figure 4: Comparison of 10-Year low-pass filtered NASST anomaly (blue) with 10-Year low-pass filtered SST anomaly averaged for the Rest of the World Ocean (red). (a) Observations (HadISST) (b) ensemble mean of HadGEM2-ES All Forcings. Green shading: 1 std of ensemble spread for low-pass filtered NASST anomaly; yellow shading: 1 std of ensemble spread for low-pass filtered SST anomaly averaged for the Rest of the World Ocean. (c) low-pass filtered NASST anomaly from HadGEM2-ES All Forcings (blue) and observations (blue dash line) (d) low-pass filtered SST anomaly averaged for the Rest of the World Ocean from HadGEM2-ES All Forcings (red) and observations (red dash line). The color shadings in (c,d) are the same as in (b).

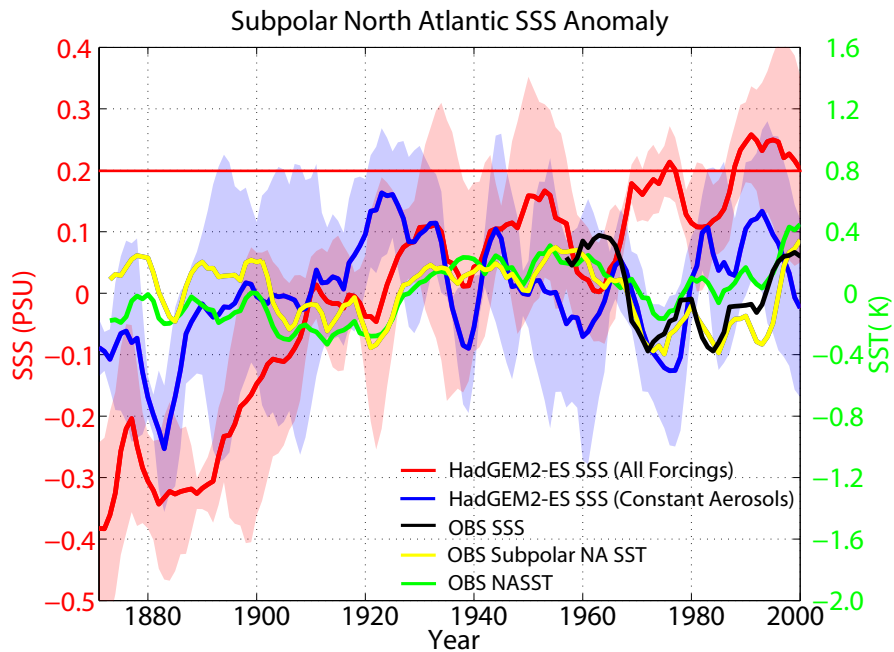


Figure 5: Subpolar North Atlantic SSS anomaly (60°W - 0°E , 50 - 65°N). Red Line: subpolar North Atlantic SSS anomaly from ensemble mean of HadGEM2-ES All Forcings simulations; Blue Line: subpolar North Atlantic SSS anomaly from ensemble mean of HadGEM2-ES Constant Aerosols simulation. Black Line: observed subpolar North Atlantic SSS anomaly (pentadally averaged), relative to 1957-2000 mean. Yellow Line: observed subpolar North Atlantic SST anomaly, relative to 1871-2000 mean. Green Line: observed North Atlantic basin-averaged NASST anomaly, relative to 1871-2000 mean. Thin red line: marking the 0.2PSU difference in the climatological mean subpolar North Atlantic SSS over the entire period 1871-2000 between HadGEM2-ES All Forcings and Constant Aerosols.

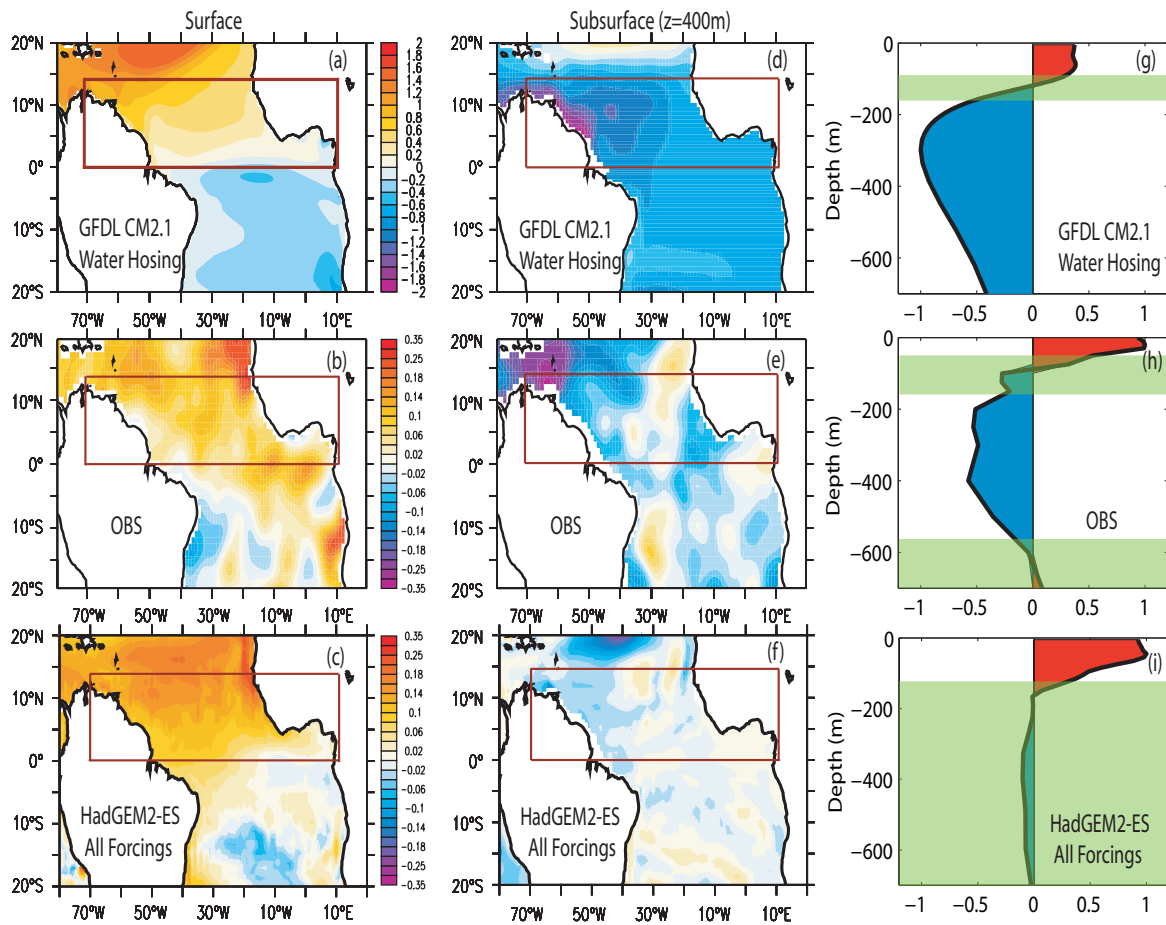


Figure 6: Regression coefficients of SST anomaly (a,b,c), subsurface ocean temperature anomaly ($z=400$) (d,e,f), and averaged Tropical North Atlantic (TNA) ocean temperature anomaly at different depths (g,h,i) onto the time series of the TNA SST anomaly, corresponding to 1 standard deviation of the TNA SST anomaly. (a, d, g) ensemble mean from water hosing experiments using GFDL CM2.1, year 1-60. (b, e, h) Using 10-year low-pass filtered observed data (OBS, 1955-2000) (c, f, i) Using 10-year low-pass filtered modeled ensemble mean from HadGEM2-ES All Forcings simulations, 1955-2000. The long-term trends have been removed for OBS and HadGEM2-ES. The brown box shows the TNA domain ($0-14^{\circ}\text{N}$ and $70^{\circ}\text{W}-0^{\circ}\text{E}$) that is used for area average. (g,h,i) are normalized by the maximum absolute value of each regression respectively, and the green shading covers depths that are not statistically significant at the 90% level of non-zero correlation using the 2-tailed Student's t -test.